Available online at www.sciencedirect.com
ScienceDirect
Polyhedron 25 (2006) 2755–2763
POLYHEDRON
www.elsevier.com/locate/poly

Synthesis, crystal structures and multinuclear NMR spectroscopy of copper(I) complexes with benzophenone thiosemicarbazone

Tarlok S. Lobana [a,*], Sonia Khanna [a], Ray J. Butcher [b], A.D. Hunter [c], M. Zeller [c]

[a] Department of Chemistry, Guru Nanak Dev University, Amritsar 143 005, India
[b] Department of Chemistry, Horward University, Washington, DC 20059, USA
[c] Department of Chemistry, 1 University Plaza, Youngstown State University, Youngstown, OH 44555 3663, USA

Received 21 February 2006; accepted 2 April 2006
Available online 25 April 2006

Abstract

Reactions of benzophenone thiosemicarbazone (Hbztsc, $Ph_2C{=}N\text{-}NH\text{-}C(=S)\text{-}NH_2$) with copper(I) chloride/bromide in the presence of two moles of PPh_3, formed monomeric tetrahedral complexes, $[CuX(\eta^1\text{-S-Hbztsc})(PPh_3)_2]\cdot CH_3CN$ (X = Cl, **1**; Br, **2**). It did not form similar complex with copper(I) iodide; rather it formed a trigonal planar complex $[CuI(\eta^1\text{-S-Hbztsc})_2]$ (**3**) with two moles of Hbztsc in absence of PPh_3. All the complexes have been characterized with the help of elemental analyses, IR, ^1H, ^{13}C, and ^{31}P NMR spectroscopy, and single crystal X-ray crystallography. The crystal structure of ligand is also described. In all the complexes, benzophenone thiosemicarbazone is acting as a neutral S donor ligand in η^1-S bonding mode. NMR data support that the complexes remain stable in solution phase.

1. Introduction

The chemistry of thiosemicarbazones has received considerable attention in view of their variable bonding modes, promising biological implications, structural diversity and ion sensing ability [1–7]. Another reason is easy access to their synthesis by modifying parent aldehyde or ketone used for synthesis or by substitution at C^2 or N^1 atoms. Chart 1 shows various bonding modes of neutral thiosemicarbazones. As regards biological implications, thiosemicarbazone complexes of copper(II) have been intensively investigated for antiviral, antibacterial, antitumour, and antifungal activity and inhibitory action is attributed to their chelating properties [8–18]. While structural chemistry of copper(II) has been well investigated [20], corresponding complexes of copper(I) are limited [19–27]. In case of copper(I), neutral thiosemicarbazones have exhibited different bonding modes: η^1-S (mode A) [19–24], μ_2-S (mode B) [24a], N^3,S-chelation (mode C) [25,26], N^3,S-chelation-cum-S-bridging (mode D) [25] (Scheme 1) and in the anionic form, there is only N^2,S-chelation-cum S-bridging (mode E) [27].

In the literature, the reported complexes of thiosemicarbazones have R = Ph, pyridyl, CH_3, etc. and R′ = H, CH_3, etc. (Chart 2) [1–4,8–41]. In other words, there is no complex of copper(I) structurally characterized with both R and R′ = Ph, or any other aryl group [8–18]. In the present work, we report the synthesis, multinuclear NMR spectroscopy and crystal structures of copper(I) halide complexes, $[CuCl(\eta^1\text{-S-Hbztsc})(PPh_3)_2]$ (**1**), $[CuBr(\eta^1\text{-S-Hbztsc})(PPh_3)_2]$ (**2**) and trigonal complex $[CuI(\eta^1\text{-S-Hbztsc})_2]$ (**3**). The crystal structure of ligand is also reported.

2. Experimental

2.1. Materials and techniques

Copper(I) halides were prepared by reducing an aqueous solution of $CuSO_4\cdot 5H_2O$ with SO_2 in the presence of NaX (X = Cl, Br, I) in H_2O [42]. Ph_3P was procured from Aldrich Chemicals Ltd. and used as such. C, H and N analysis were obtained with Thermoelectron FLASHEA1112 CHNS

* Corresponding author. Tel.: +91 183 257604; fax: +91 183 2 258820.
E-mail address: tarlokslobana@yahoo.co.in (T.S. Lobana).

0277-5387/$ - see front matter © 2006 Elsevier Ltd. All rights reserved.
doi:10.1016/j.poly.2006.04.006

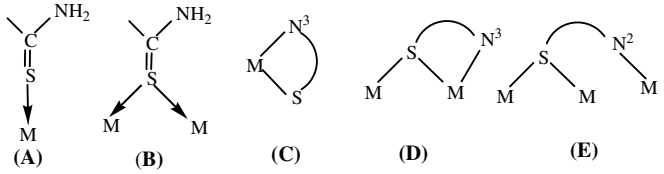

Chart 1.

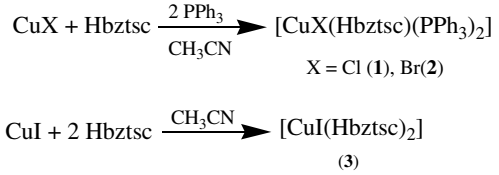

Scheme 1.

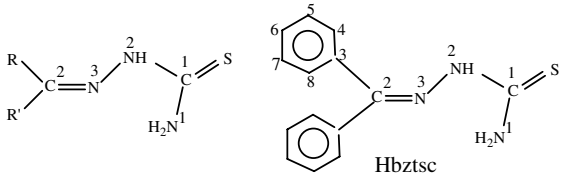

Chart 2.

analyzer. Infrared spectra were recorded as KBr pellets in the range 4000–200 cm^{-1} on Pye–Unicam SP-3-300 spectrophotometer. The melting points were determined with a Gallenkamp electrically heated apparatus. ^1H NMR were recorded on a JEOL AL-300 FT spectrometer operating at a frequency of 300 MHz using $CDCl_3$ as solvent with TMS as internal reference. ^{13}C NMR spectra were recorded at a frequency of 200 MHz using $CDCl_3$ as solvent and TMS as an internal reference. ^{31}P NMR spectra were recorded on a Bruker ACP-300 spectrometer operating at a frequency of 121.5 MHz with $(CH_3O)_3P$ as external reference set at zero value.

2.2. Preparation of ligand (Hbztsc)

To a solution of thiosemicarbazide (2.5 g, 0.027 mol) in hot distilled water (50 mL) and glacial acetic acid (5 mL), was slowly added benzophenone (4.99 g, 0.027 mol) dissolved in methanol (30 mL). The contents were refluxed for 30 h. and the clear solution containing yellowish orange oily layer, was poured in a beaker and stirred vigorously with a glass rod. The yellow solid formed was dried and recrystallised using methanol. Slow evaporation of the solution gave clear yellow crystals. (25%, m.p. 160–162 °C). *Anal.* Calc. for $C_{14}H_{13}N_3S$: C, 65.79; H, 5.09; N, 16.45. Found: C, 65.66; H, 4.93; N, 16.25%. Main IR peaks (KBr, cm^{-1}): ν(N–H) 3412 s, 3346 s, 3247 m, (–NH_2–) 3151 s (–NH–); 1608b, 1437b ν(C=N) + δNH_2 + ν(C=C); 1070 s, 1026 s, 846 s (thioamide moiety). ^1H NMR ($CDCl_3$, δ ppm) 8.68 (–N^2H), 7.81 s, 6.45 sb (N^1H_2), 7.27–7.61 m (Ph). ^{13}C NMR ($CDCl_3$, δ ppm, J, Hz): 178.8 (C^1); 151.0 (C^2); 136.3, 131.0 (C^3); 130.3, 130.23 (C^6); 129.86, 127.7 ($C^{4,8}$); 128.4 ($C^{5,7}$).

2.3. Synthesis of complexes

2.3.1. [CuCl(η^1-S-Hbztsc)(PPh_3)$_2$] · CH_3CN (1)

To a solution of CuCl (0.025 g, 0.25 mmol) in dry acetonitrile (15 mL) was added solid Hbztsc (0.064 g, 0.25 mmol) and the contents were stirred for 3 h at room temperature. During stirring, a yellow solid formed was separated. To this solid suspended in acetonitrile was added PPh_3 (0.132 g, 0.50 mmol) and stirring was continued for further 1 h followed by refluxing for 10 min. Clear light yellow solution formed was filtered and allowed to evaporate at room temperature. Slow evaporation of solution gave clear light yellow crystals. Complex is soluble in chloroform, dichloromethane and hot acetonitrile (60%, m.p. 182–184 °C). *Anal.* Calc. for $C_{50}H_{43}ClCuN_3P_2S \cdot CH_3CN$: C, 67.83; H, 5.00; N, 6.08. Found: C, 67.58; H, 5.04; N, 5.52%. Main IR peaks (KBr, cm^{-1}): ν(N–H) 3336 s, 3238 m (–NH_2–), 3144 m (–NH–); 1602 m, 1585 sh ν(C=N) + $\delta(NH_2)$ + ν(C=C); 1072 s, 1024 s, 841 s (thioamide moiety); 1093 s ν(P–C_{Ph}). ^1H NMR ($CDCl_3$, δ ppm) 9.11 b (–N^2H), 8.57 s, 6.91 s (–N^1H_2), 7.29–7.69 m (Ph + PPh_3). ^{13}C NMR ($CDCl_3$, δ ppm, J, Hz) 176.9 (C^1); 157.9 (C^2); 136.3, 131.1 (C^3); 130.4 (C^6); 129.8, 127.8 ($C^{4,8}$); 128.6 ($C^{5,7}$); 133.9 (*i*-C, PhP); 133.9 (*o*-C, $J_{P-C} = 15.1$, PhP); 129.4 (*p*-C, PhP); 128.4 (*m*-C, $J_{P-C} = 8.8$, PhP). ^{31}P NMR ($CDCl_3$, δ ppm): −112.16 ppm, $\Delta\delta(\delta_{complex} - \delta_{ligand}) = 0.991$ ppm. Compound **2** was prepared in the similar manner.

2.3.2. [CuBr(η^1-S-Hbztsc)(PPh_3)$_2$] · CH_3CN (2)

Crystals were grown from an acetonitrile solution at room temperature. Complex is soluble in chloroform, dichloromethane and hot acetonitrile (61%, m.p. 184–186 °C). *Anal.* Calc. for $C_{50}H_{43}BrCuN_3P_2S \cdot CH_3CN$: C, 64.70; H, 4.76; N, 5.80. Found: C, 64.82; H, 5.15; N, 5.31%. Main IR peaks (KBr, cm^{-1}): ν(N–H) 3344 s, 3236m (–NH_2–), 3157 m (–NH–); 1602 s, 1585 m ν(C=N) + $\delta(NH_2)$ + ν(C=C); 1025 s, 837 s (thioamide moiety); 1091 s ν(P–C_{Ph}). ^1H NMR ($CDCl_3$, δ ppm) 9.02 b (–N^2H), 8.46 s (–N^1H_2), 7.20–7.66 m (–N^1H_2 + Ph + PPh_3). ^{13}C NMR ($CDCl_3$, δ ppm, J, Hz) 176.6 (C^1); 151.7 (C^2); 136.3, 131.1 (C^3); 130.4 (C^6); 129.5, 127.8 ($C^{4,8}$); 128.5 ($C^{5,7}$); 133.4 (*i*-C, PhP), 133.9 (*o*-C, $J_{P-C} = 14.7$, PhP),129.4 (*p*-C, PhP), 128.4 (*m*-C, $J_{P-C} = 9.1$, PhP). ^{31}P NMR ($CDCl_3$, δ ppm): −112.73, $\Delta\delta(\delta_{complex} - \delta_{ligand}) = 0.427$ ppm.

2.3.3. [CuI(η^1-S-Hbztsc)$_2$] (3)

To a solution of CuI (0.025 g, 0.13 mmol) in dry acetonitrile (20 mL) was added solid Hbztsc (0.067 g, 0.26 mmol) and contents were stirred for 4 h. Clear yellow solution was filtered and allowed to evaporate at room temperature. Slow evaporation of solution gave clear

yellow crystalline needles. Complex is soluble in chloroform, dichloromethane and hot acetonitrile. (68.5%, m.p. 210–212 °C). *Anal.* Calc. for $C_{28}H_{26}CuIN_6S_2$: C, 47.92; H, 3.71; N, 11.98. Found: C, 48.53; H, 3.84; N, 11.81%. Main IR peaks (KBr, cm^{-1}): ν(N–H) 3390 s, 3346 s, 3223 m (–NH_2–) 3149 s (–NH–); 1595 sh, 1583 m, 1500 m ν(C=N) + δ(NH) + ν(C=C); 1072 s, 1026 s, 831 s (thioamide moiety). ^{1}H NMR ($CDCl_3$, δ ppm), 8.78 s (–N^2H), 8.06 sb (–N^1H_2), 7.28–7.60 m (N^1H_2 + Ph).

2.4. X-ray crystallography

Suitable light yellow crystals of Hbztsc and compounds **1**, **2** and **3** were mounted on an automatic Enraf Nonius CAD-4 diffractometer equipped with graphite monochromator and Mo Kα radiation ($\lambda = 0.71073$ Å). The unit cell dimensions and intensity data were measured at 93 K for Hbztsc, **1**, **2** and 100 K for **3**. The structures were solved by direct methods and refined by full matrix least squares method based on F^2. All nonhydrogen atoms were refined anisotropically using XCAD-49 (data reduction) and SHELXL. The hydrogen atoms were calculated using structure factor calculations in their idealized positions. The crystallographic data is summarized in Table 1.

3. Results and discussion

3.1. Synthesis and infrared spectroscopy

Reaction of copper(I) chloride/copper(I) bromide with benzophenone thiosemicarbazone (Hbztsc, Ph_2C=N–NH–C(=S)–NH_2) in the molar ratio of 1:1 in MeCN formed an insoluble product of stoichiometry {CuX-(Hbztsc)} which after addition of two moles of PPh_3 yielded a monomeric tetrahedral complex [CuX(Hbztsc)(PPh_3)$_2$] (X = Cl, **1**; Br, **2**) (Scheme 1). Reaction of copper(I) iodide with Hbztsc in the presence of two moles of PPh_3 did not form similar complex, rather it formed a known cubane complex, {$Cu_4I_4(PPh_3)_4$}. However copper(I) iodide with Hbztsc in MeCN in the absence of PPh_3, formed a trigonal complex [CuI(Hbztsc)$_2$] (**3**). All these complexes have melting points in the range of 182–210 °C. Complexes **1** and **2** are readily soluble in chloroform while **3** is sparingly soluble.

The IR spectra of ligand (Hbztsc) shows ν(N–H) in the range of 3412–3247 cm^{-1} (–NH_2) and at 3151 s (–NH–). In all the complexes, ν(N–H) ranges from 3390–3236 cm^{-1} (–NH_2) and 3160–3140 cm^{-1} (–NH–). It suggests the neutral monodentate (η^1-S) nature of ligand Hbztsc. The thioamide bands ν(C–S) + ν(C–N) appear in the range of 846–1085 cm^{-1} in Hbztsc. These modes appear in the region of 830–1090 cm^{-1} in the complexes. Medium to broad peaks appear at 1608 b, 1473 b cm^{-1} in free ligand corresponding to ν(C=N), δ(NH_2) and ν(C=C). However, they appear in the range of 1500–1605 cm^{-1} in all the complexes. A characteristic ν(P–C_{Ph}) peak at 1093 s cm^{-1} in (**1**) and 1091 s cm^{-1} in (**2**) confirms the presence of PPh_3 in the coordinated form in the complexes.

3.2. Crystal structures of ligand and complexes *1–3*

The atomic numbering schemes for molecular structures of ligand and complexes **1**, **2** and **3** are shown in Figs. 1–4 and the selected bond lengths and angles are given in Table 2.

Table 1
Crystallographic data for compounds **1**, **2**, **3** and ligand

	1	**2**	**3**
Empirical formula	$C_{50}H_{43}ClCuN_3P_2S \cdot CH_3CN$	$C_{50}H_{43}BrCuN_3P_2S \cdot CH_3CN$	$C_{28}H_{26}CuIN_6S_2$
MW	919.92	964.38	701.11
Crystal colour	yellow	yellow	yellow
Crystal system	triclinic	triclinic	monoclinic
Space group	$P\bar{1}$	$P\bar{1}$	$P2/c$
a (Å)	12.3639(8)	10.356(7)	16.4147(14)
b (Å)	13.9423(8)	14.480(11)	6.1106(17)
c (Å)	14.8040(9)	17.684(13)	31.3870(7)
V (Å^3)	2255.8(2)	2311(3)	2893.2(8)
α (°)	113.9130(10)	66.206(12)	90
β (°)	100.6420(10)	79.346(14)	113.22
γ (°)	94.9190(10)	72.729(13)	90
Z	2	2	4
D (Mg m^{-3})	1.354	1.386	1.610
μ(Mo Kα) (mm^{-1})	0.702	1.492	1.995
Reflections collected	18082	18915	10863
Unique reflections, R_{int}	10732, 0.0450	10975, 0.0365	10897, 0.0000
Final R indices R_1 and wR_2	0.0490, 0.1006	0.0502, 0.114	0.0379, 0.0937

Crystal data for $C_{14}H_{13}N_3S$: 255.33; monoclinic; $C2/c$; $a = 26.5443(16)$ Å; $b = 6.0935(4)$ Å; $c = 16.7931(10)$ Å; $V = 2649.2(3)$ Å^3; $\alpha = 90°$; $\beta = 102.7580(10)°$; $\gamma = 90°$; $V = 2649.2(3)$ Å^3; $Z = 8$; $D = 1.280$ Mg m^{-3}; μ(Mo Kα) (mm^{-1}) = 0.229; reflections collected = 9934; unique reflections = 3227; $R_{int} = 0.0297$; $R = 0.0453$.

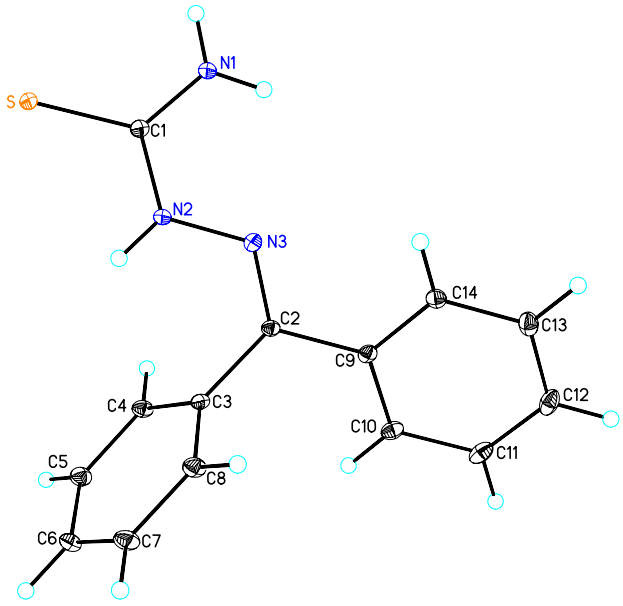

Fig. 1a. The structure of ligand (Hbztsc) with numbering scheme.

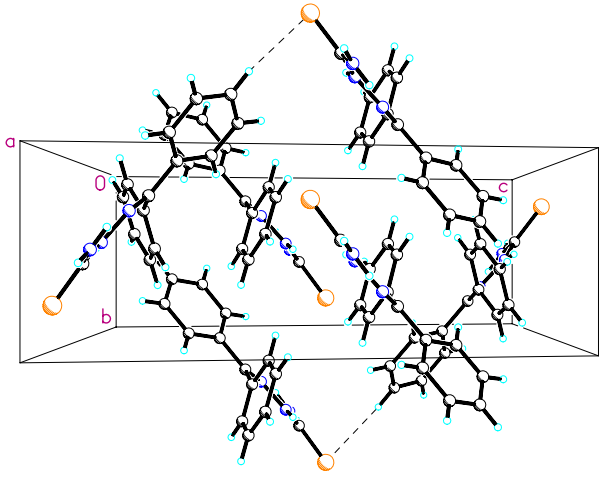

Fig. 1b. Packing diagram of the ligand (Hbztsc).

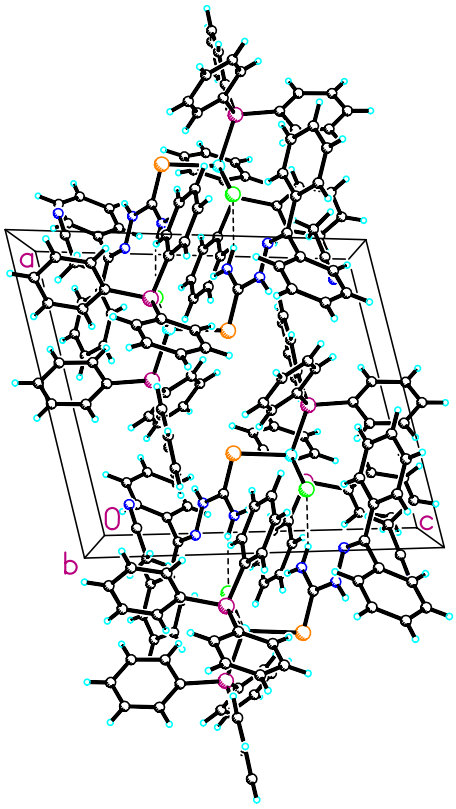

Fig. 2b. Packing diagram of [CuCl(η^1-S-Hbztsc)(PPh_3)$_2$] · CH_3CN (**1**).

3.2.1. Ligand

The ligand (Hbztsc) crystallized in the monoclinic space group *C*2/*c*. The S and the hydrazinic N(3) atoms are *trans* with respect to C(1)–N(2) bond and thus ligand has *E* configuration. The C(1)–S bond distance, 1.6866(17) Å is close to a double bond, and comparable with ca.1.69 Å in salicylaldehyde thiosemicarbazone and 2-hydroxyacetophenone [43,44]; other bonds, C(2)–N(3), C(1)–N(1), C(1)–N(2), N(2)–N(3) are also comparable with the literature data

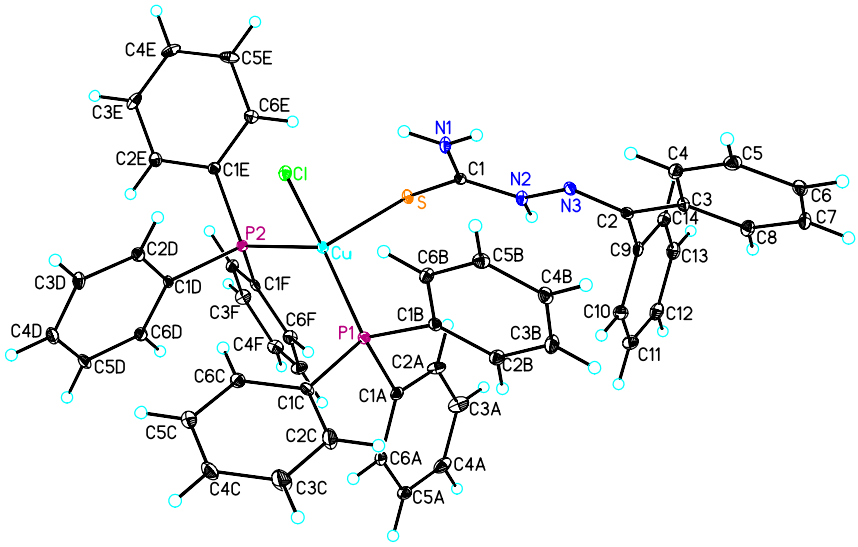

Fig. 2a. The structure of [CuCl (η^1-S-Hbztsc)(PPh_3)$_2$] · CH_3CN (**1**) with numbering scheme.

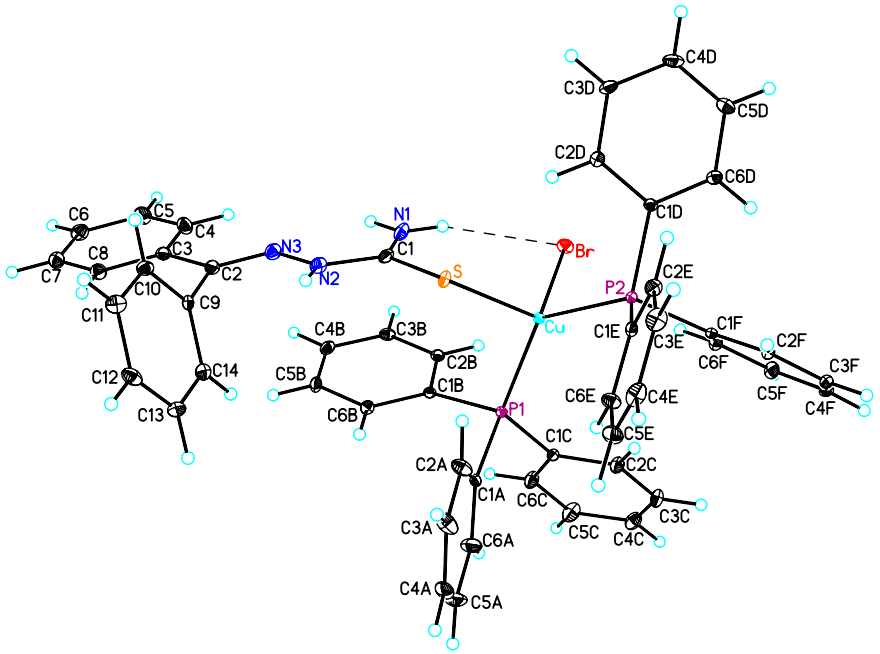

Fig. 3a. The structure of $[CuBr(\eta^1\text{-S-Hbztsc})(PPh_3)_2]\cdot CH_3CN$ (**2**) with numbering scheme.

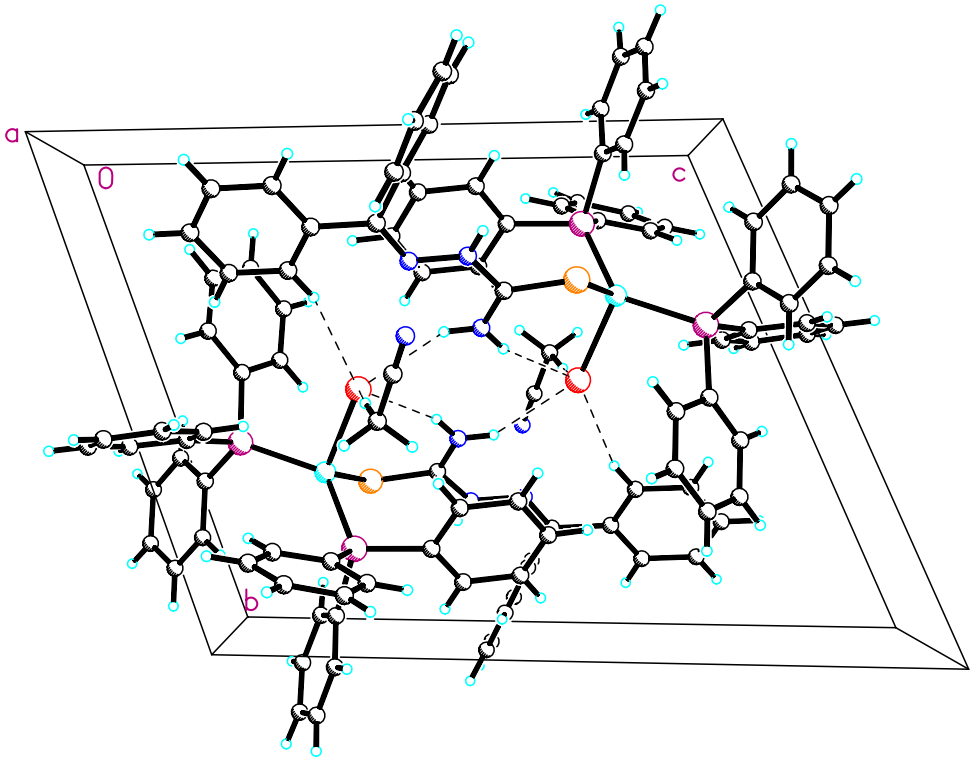

Fig. 3b. Packing diagram of $[CuBr(\eta^1\text{-S-Hbztsc})(PPh_3)_2]\cdot CH_3CN$ (**2**).

[43–45]. There is a moderately strong intermolecular N(1)–H(1B)···S* bond [2.49 Å] {cf. sum of van der Waals radii of H and S, 3.0 Å [46]} and a long range C–H_{Ph}···S intermolecular hydrogen bonding leading to formation of dimer as shown in Fig. 1b.

3.2.2. Complexes *1–3*

Complexes **1** and **2** have the triclinic space groups, while complex **3** has monoclinic space group. The E-configuration of free ligand is unchanged in the complexes. In complex **1**, copper is bonded to one S atom of the ligand

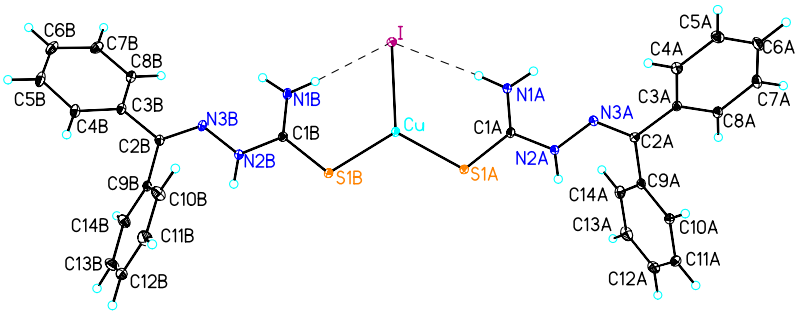

Fig. 4a. The structure of $[CuI(\eta^1\text{-S-Hbztsc})_2]$ (**3**) with numbering scheme.

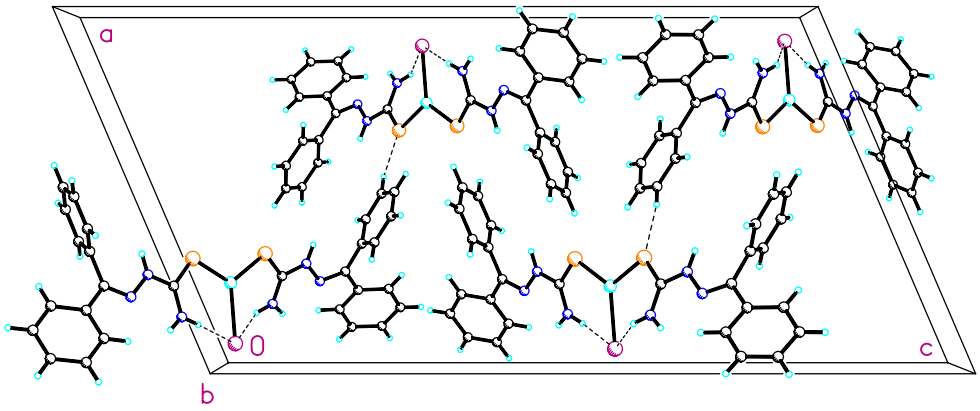

Fig. 4b. Packing diagram of $[CuI(\eta^1\text{-S-Hbztsc})_2]$ (**3**).

(Hbztsc) with Cu–S bond distance of 2.3606(8) Å; two P atoms from PPh_3 ligands {Cu–P(1), 2.2665(8) Å; Cu–P(2), 2.2505(8) Å}, and one chlorine atom at Cu–Cl bond distance of 2.3757(7) Å. Complex **2** has similar bond parameters, viz., Cu–S, 2.3542(17) Å; Cu–P(1), 2.2749 (17) Å; Cu–P(2), 2.2552(16) Å; Cu–Br, 2.4863(12) Å. The angles around Cu lie in the ranges, 102.55(3)–126.00(3)° and 99.49(6)–131.56(4)° in compounds **1** and **2**, respectively, with P(2)–Cu–P(1) being the largest, and P(2)–Cu–X {X = Cl, Br} being the smallest. This reveals a distorted tetrahedral geometry around Cu atom in both the complexes. Finally in complex **3**, each Cu is bonded to two S atoms of two Hbztsc ligands with Cu–S distances of 2.2269(7), 2.2321(7) Å, and to one iodine atom with Cu–I bond distance of 2.5441(4) Å. The angles around Cu range from 118.95(2)° to 121.42(2)°, indicating a trigonal geometry around copper center. The C–S bond distances in these complexes are marginally longer vis-à-vis free ligand, and reveal weakening of pπ–pπ bond. It may be noted that trends of variation in Cu–P, Cu–S and C–S distances are analogous to the literature values [19,21,24a]. The absence of PPh_3 in trigonal planar complex **3** makes a stronger Cu–S bond. Further, Cu–X distances in the complexes are much less than the sum of the ionic radii of Cu^+ and X^- (Cu^+, Cl^-, 2.58 Å; Cu^+, Br^-, 2.73 Å; Cu^+, I^-, 2.97 Å [46]).

In the solid state, amino (–HN^1H) hydrogen atom of thiosemicarbazone is involved in hydrogen bonding in all the complexes (Table 3). In complex (**1**), one hydrogen of amino group is engaged in intramolecular –$HN^1H\cdots$Cl hydrogen bonding while other hydrogen is involved in intermolecular –$HN^1H\cdots$Cl hydrogen bonding forming a dimer (Fig. 2b). Similar trend of bonding is seen in complex **2** except for the presence of additional long range C–H_{Ph}(Hbztsc)$\cdots$Br contact resulting in the formation of 8 membered ring in the center of the dimer. Two molecules of CH_3CN are present as solvent of crystallization per unit cell in the crystal packing but are not involved in any sort of hydrogen bonding at all and also do not appear in the analysis (Fig. 3b). However, in complex **3**, one hydrogen of amino group is engaged in intramolecular –$HN^1H\cdots$I hydrogen bonding while other hydrogen remains free. In addition, long range intermolecular C–H_{Ph}(Hbztsc)$\cdots$S hydrogen bonding is present forming a dimer (Fig. 4b).

A comparison of P–Cu–P, S–Cu–X and Cu–S–C bond angles is made for various Cu^I-complexes with analogous thiosemicarbazones (Table 4). The groups at C^2 carbon appear to play significant role in affecting the above angles which are correlated with the electronegativity of halogen atoms. When py, H (**4**–**6**) [24a] ; and Ph, H (**7**, **8**) [24a] are bonded to C^2 carbon, angles Cu–S–C and S–Cu–X increase with change in X from chloride to iodide; and the corresponding P–Cu–P bond angles decrease. The halogens are engaged in intramolecular –$N^2H\cdots$X, or –$N^1H_2\cdots$X hydrogen bonds and strengths of these bonds obviously vary with the electronegativity of halogen atoms. Chart 3 exhibits how the amino and imino hydrogen atoms

Table 2
Selected bond distances (Å) and bond angles (°) for ligand (Hbztsc) and complexes **1**, **2** and **3**

Bond distances			
Hbztsc			
S–C(1)	1.6866(17)	N(3)–C(2)	1.289(2)
N(1)–C(1)	1.321(2)	C(2)–C(3)	1.496(2)
N(2)–C(1)	1.358(2)	C(2)–C(9)	1.481(2)
N(2)–N(3)	1.3766(19)		
1			
Cu–S	2.3606(8)	N(2)–C(1)	1.351(3)
Cu–P(1)	2.2665(8)	N(2)–N(3)	1.374(3)
Cu–P(2)	2.2505(8)	N(2)–C(2)	1.296(4)
Cu–Cl	2.3757(7)	C(2)–C(3)	1.479(4)
S–C(1)	1.702(3)	C(2)–C(9)	1.495(4)
N(1)–C(1)	1.314(3)		
2			
Cu–S	2.3542(17)	N(2)–C(1)	1.395(4)
Cu–P(1)	2.2749(17)	N(2)–N(3)	1.357(4)
Cu–P(2)	2.2552(16)	N(3)–C(2)	1.291(5)
Cu–Br	2.4863(12)	C(2)–C(3)	1.499(5)
S–C(1)	1.699(4)	C(2)–C(9)	1.513(5)
N(1)–C(1)	1.292(5)		
3			
Cu–I	2.5441(4)	N(2A)–N(3A)	1.378(3)
Cu–S(1A)	2.2269(7)	N(2B)–N(3B)	1.378(3)
Cu–S(1B)	2.2321(7)	N(3A)–C(2A)	1.288(3)
S(1A)–C(1A)	1.712(7)	N(3B)–C(2B)	1.289(3)
S(1B)–C(1B)	1.708(2)	C(2A)–C(3A)	1.479(3)
N(1A)–C(1A)	1.306(3)	C(2A)–C(9A)	1.493(3)
N(1B)–C(1B)	1.306(3)	C(2B)–C(3B)	1.480(3)
N(2A)–C(1A)	1.346(3)	C(2B)–C(9B)	1.493(3)
N(2B)–C(1B)	1.352(3)		
Bond angles			
Hbztsc			
C(1)–N(2)–N(3)	119.71(13)	N(2)–C(1)–S	118.58(12)
C(2)– N(3)–N(2)	117.42(14)	N(3)–C(2)–C(3)	124.33(14)
N(1)–C(1)–S	124.71(13)	N(3)–C(2)–C(9)	116.68(14)
1			
P(2)–Cu–P(1)	126.00(3)	C(1B)–P(1)–Cu	115.40(9)
P(2)–Cu–S	106.49(3)	C(1C)–P(1)–Cu	117.17(10)
P(1)–Cu–S	107.17(3)	C(1A)–P(1)–Cu	112.85(10)
P(2)–Cu–Cl	102.55(3)	C(1F)–P(2)–Cu	117.60(9)
P(1)–Cu–Cl	106.96(3)	C(1D)–P(2)–Cu	113.17(9)
S–Cu–Cl	106.21(3)	C(1E)–P(2)–Cu	114.27(10)
C(1)–S–Cu	101.93(10)		
2			
P(2)–Cu–P(1)	131.56(4)	C(1B)–P(1)–Cu	109.40(10)
P(2)–Cu–S	104.64(4)	C(1C)–P(1)–Cu	120.06(11)
P(1)–Cu–S	103.34(4)	C(1A)–P(1)–Cu	115.35(12)
P(2)–Cu–Br	99.49(6)	C(1F)–P(2)–Cu	116.31(11)
P(1)–Cu–Br	105.27(6)	C(1D)–P(2)–Cu	112.30(11)
S–Cu–Br	112.38(4)	C(1E)–P(2)–Cu	117.45(11)
C(1)–S–Cu	108.19(12)		
3			
S(1A)–Cu–S(1B)	119.62(3)	C(1A)–N(2A)–N(3A)	118.8(2)
S(1A)–Cu–I	121.42(2)	C(2A)–N(3A)–N(2A)	117.6(2)
S(1B)–Cu–I	118.95(2)	C(1B)–N(2B)–N(3B)	118.0(2)
C(1A)–S(1A)–Cu	110.62(8)	C(2B)–N(3B)–N(2B)	117.6(2)
C(1B)–S(1B)–Cu	110.30(9)	N(1A)–C(1A)–(N2A)	117.6(2)

are involved in hydrogen bonding with halogens. A stronger $-N^2H\cdots X$ or $-N^1H_2\cdots X$ hydrogen bond shortens the Cu–S–C bond angle, which leads to opening of P–Cu–P angle. The trend for *p*-HOC_6H_5, H groups (**9**, **10**) [21] bonded to C^2 is similar except for S–Cu–X which decreased and this may be due to the packing effect or presence of solvent of crystallization. Due to rigidity of isatin groups (**11**, **12**) [19], the above trends are less significant.

The most significant observation is found when two Ph groups are bonded to C^2 carbon. Both Cu–S–C and S–Cu–X angles increase as noted for above complexes. However, P–Cu–P angle increases with change in halide from chloride (121°) to bromide (131°) in complexes **1** and **2**, unlike the expected decreasing trend. The increased P–Cu–P bond angle in complex **2** is due to the steric effect of two Ph groups at C^2 carbon with large bromide group. In case of still bulky iodide group in complex **3**, this steric effect becomes very large and this explains lack of formation copper(I) iodide complex containing PPh_3 ligands similar to **1** or **2**.

3.3. NMR spectroscopy

The ^1H NMR of ligand Hbztsc in $CDCl_3$ shows a singlet at 8.68 ppm (N^2H), which shifted downfield to 9.11 ppm in complex **1**, 9.02 ppm in complex **2** and 8.78 ppm in complex **3**. This is in accordance with the coordination behaviour of thiosemicarbazones [24a], and its presence in the spectra of complexes indicates that N^2H protons are not deprotonated. The N^1H_2 protons of free ligand Hbztsc exhibit two sets of signals, one broad peak (unresolved) at 6.45 ppm and a doublet at 7.81 ppm. This can be attributed to the restricted rotation about C^1–N^1 bond axis due to delocalization of lone pairs of electrons on N^1H_2 nitrogen. A pair of broad signals corresponding to N^1H_2 protons appear downfield at 6.91 ppm and 8.56 ppm in complex **1**. However, a single broad signal is observed at 8.47 ppm in complex **2** and 8.06 ppm in complex **3**. The second signal is probably obscured by the protons of phenyl rings. This may be attributed to intermolecular as well as intramolecular $-HN^1H\cdots X$ (X = Cl, Br, I) hydrogen bonding in the solid state which may be operative even in the solution phase. The phenyl protons in free ligand show a series of multiplets in the region of 7.27–7.61 ppm. Ph_3P signals in the complexes merged with the signals of phenyl protons of ligand and show a series of doublets and multiplets in the region of 7.29–7.69 ppm in **1** and 7.20–7.66 ppm in **2**. In complex **3**, phenyl protons appeared unchanged at 7.28–7.60 ppm.

The ^{13}C NMR spectra provide more convincing information about the monodentate behaviour of Hbztsc moiety in the complexes. The C^1 carbon signal appears at δ 176.9 ppm in **1** and at δ 176.5 ppm in **2**, which are upfield relative to the free ligand (δ 178.8 ppm). Further, C^2 carbon signal at δ 157.9 ppm in **1** and δ 151.7 ppm in **2** shifts downfield relative to the free ligand (δ 150.98 ppm), the former carbon showing more pronounced shift. This behaviour is similar to that observed for related complexes

Table 3
Hydrogen bonds (Å) for complexes **1**–**3**

Complex no.	D–H...A	*d*(D–H)	*d*(H...A)	*d*(D...A)	∠(DHA)
1	N(1)–H(1A)...Cl#1	0.88	2.44	3.230(2)	149.3
	N(1)–H(1B)...Cl	0.88	2.54	3.281(3)	142.7
2	N(1)–H(1A)...Br#1	0.88	2.63	3.407(4)	147.3
	N(1)–H(1B)...Br	0.88	2.64	3.494(4)	163.1
3	N(1A)–(H1AA)...I#1	0.88	3.08	3.570(2)	117.2
	N(1A)–H(1AB)...I	0.88	2.65	3.503(2)	164.0
	N(1B)–H(1BA)...I#2	0.88	3.19	3.764(2)	125.2
	N(1B)–H(1BB)...N(1A)#2	0.88	2.67	3.157(3)	116.2
	N(1B)–H(1BB)...I	0.88	2.75	3.509(2)	145.7

Table 4
Comparison of bond angles (°) of complexes **1**–**3** with related complexes

S. no.	Ligand	Complexes	C(1)–S–Cu	P–Cu–P	S–Cu–X	Hydrogen bonding (H···X)
	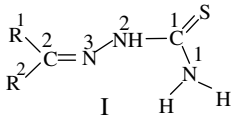 I					
	R^1, R^2					
1	Py, H	Cl (**4**)	103.13(8)	120.92(2)	103.13(8)	–NH–
		Br (**5**)	105.82(15)	122.39(5)	107.76(4)	–NH–
		I (**6**)	115.85(18)	117.21(5)	113.41(4)	$–NH_2–$
2	Ph, H	Br (**7**)	110.52(8)	123.31(2)	109.93(18)	$–NH_2–$
		I (**8**)	115.73(7)	118.11(2)	115.42(2)	–NH–
3	*p*-OHC_6H_5, H	Br (**9**)	107.0(11)	135.4(1)	114.81(9)	–NH–
		I (**10**)	112.1(4)	123.1(1)	110.18(9)	–NH–
4	Ph, Ph	Cl (**1**)	101.93(10)	126.00(3)	108.22(17)	$–NH_2–$
		Br (**2**)	108.19(12)	131.56(4)	112.38(4)	$–NH_2–$
		I (**3**)	110.62(8), 110.30(9)		121.42(2), 118.95(2)	$–NH_2–$
5	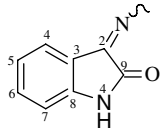	Br (**11**)	113.30(12)	121.97(3)	109.22(3)	$–NH_2–$
		I (**12**)	115.50(2)	124.09(5)	112.13(4)	$–NH_2–$

(**1**)–(**3**) this work; [CuCl(Hpytsc)$(PPh_3)_2$] (**4**) [CuBr(Hpytsc)$(PPh_3)_2$] (**5**) [CuI(Hpytsc)$(PPh_3)_2$] (**6**) (Hpytsc = pyridine-2-carbaldehyde thiosemicarbazone), [CuBr(Hbtsc)$(PPh_3)_2$] (**7**), [CuI(Hbtsc)$(PPh_3)_2$]. (**8**) (Hbtsc = Benzaldehyde thiosemicarbazone) [24a]; [CuBr(L)$(PPh_3)_2$] (**9**), [CuI(L)$(PPh_3)_2$] (**10**) (L = 4 hydroxybenzaldehyde thiosemicarbazone) [21]; [CuBr(H_2istsc)$(PPh_3)_2$] (**11**); [CuI(H_2istsc)$(PPh_3)_2$] (**12**) (H_2istsc = Isatin-3-carbaldehyde thiosemicarbazone) [19].

[24a]. C^3 carbon in free ligand shows a pair of low intensity signals at δ 136.3 ppm and δ 131.0 ppm. This can be attributed to the fact that the two phenyl rings at C^2 carbon in the free ligand as well as in complexes are not coplanar rather at an angle with respect to each other. Thus carbon atoms of two phenyl rings at C^2 carbon are in different chemical environments due to different spatial arrangement of phenyl rings, also revealed by the X-ray structure of the ligand (Fig. 1a). Similarly, $C^{4,8}$ and C^6 carbon atoms show pairs of signals at δ 129.8, 127.7 ppm and δ 130.3, 130.2 ppm, respectively. A single broad signal at δ 128.4 ppm is observed for $C^{5,7}$ carbons. Similar signals are observed for ligand ring carbons (C^3,$C^{4,8}$,$C^{5,7}$,C^6) in the complexes **1** and **2** showing no significant shift. Various signals due to *ipso* carbon, *ortho*, *meta* and *para* carbons of phosphine ligands are well resolved in both the complexes. The *i*-C, *ortho*, *meta* and *para* carbon signals of Ph rings of

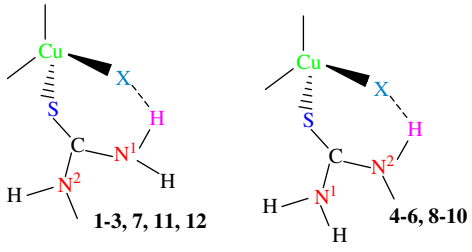

Chart 3.

PPh_3 in **1** appear as separate and are similar to the corresponding signals in **2**.

The ^{31}P NMR signal of free Ph_3P appears at −113.153 ppm. A single broad signal is observed in the complexes **1** and **2** indicating the equivalence of two PPh_3 groups. This signal shifted downfield to −112.16 ppm in **1** and −112.73 ppm in **2** with coordination shifts ($\delta_{complex} - \delta_{ligand}$) of 0.99 and 0.43 ppm, respectively. Such low coordination shifts can be attributed to the equilibrium between coordinated PPh_3 and the free PPh_3 in the solution phase, and similar behaviour was observed in the literature [24b].

4. Supplementary material

Supplementary data is available from CCDC, 12 Union Road, Cambridge CB2 1EZ, UK (fax: +44 12336033; e-mail: deposit@ccdc.cam.ac.uk, or on the web www.ccdc.cam.ac.uk) on request quoting the deposition number CCDC 297906 for (**1**), 297907 for (**2**), 297908 for (**3**) and 297909 for Hbztsc.

Acknowledgements

Financial assistance from CSIR, New Delhi (F. No. 9/254(159)/2005-EMR-I) and research facilities to one of us (Sonia) by the university are gratefully acknowledged.

References

[1] D.X. West, S.B. Padhye, P.B. Sonaware, Struct. Bond. (Berlin) 76 (1991) 4.
[2] M.J.H. Campbell, Coord. Chem. Rev. 15 (1975) 279.
[3] S. Padhye, G.B. Kauffman, Coord. Chem. Rev. 63 (1985) 127.
[4] D.X. West, A.E. Liberta, S.B. Padhye, R.C. Chilate, P.B. Sonaware, A.S. Kumbhar, R.G. Yerande, Coord. Chem. Rev. 123 (1993) 49.
[5] J.S. Casas, M.S. Garcia-Tasende, J. Sordo, Coord. Chem. Rev. 209 (2000) 197.
[6] D.R. Smith, Coord. Chem. Rev. 164 (1997) 575.
[7] R.K. Mahajan, I. Kaur, T.S. Lobana, Talanta 59 (2003) 101.
[8] D.X. West, J.J. Ingram, N.M. Kozub, G.A. Bain, A.E. Liberta, Transition Met. Chem. 21 (1996) 213.
[9] E.W. Ainscough, A.M. Brodie, J.D. Ransford, J.M. Waters, J. Chem. Soc., Dalton. Trans. (1997) 1251.
[10] M.A. Ali, A.H. Mirza, A.M.S. Hossain, M. Nazimuddin, Polyhedron 20 (2001) 1045.
[11] D.X. West, M.M. Salberg, G.A. Bain, A.E. Liberta, J.-V. Martinez, S.H. Ortega, Transition Met. Chem. 21 (1996) 206.
[12] E.W. Ainscough, A.M. Brodie, J.D. Ransford, J.M. Waters, J. Chem. Soc., Dalton. Trans. (1991) 2125.
[13] M. Baldini, M.B. Ferrari, F. Bisceglie, G. Pelosi, S. Pinelli, P. Tarasconi, Inorg. Chem. 42 (2003) 2049.
[14] E.W. Ainscough, A.M. Brodie, J.D. Ransforsd, J.M. Waters, J. Chem. Soc., Dalton. Trans. (1991) 1737.
[15] M.B. Ferrari, F. Bisceglie, G. Pelosi, P. Tarasconi, R. Albertini, G.G. Fava, S. Pinelli, J. Inorg. Biochem. 89 (2002) 36.
[16] M.E. Hossain, M.N. Alam, J. Begum, M.A. Ali, M. Nazimuddin, F.E. Smith, R.C. Hynes, Inorg. Chim. Acta 249 (1996) 247.
[17] D.X. West, A.M. Stark, G.A. Bain, A.E. Liberta, Transition Met. Chem. 21 (1996) 289.
[18] M.B. Ferrari, F. Bisceglie, G. Pelosi, P. Albertini, P.P. Dall'Aglio, A. Bergamo, G. Sava, S. Pinelli, J. Inorg. Biochem. 98 (2004) 301.
[19] T.S. Lobana, Rekha, B.S. Sidhu, A. Castineiras, E. Bermejo, T. Nishioka, J. Coord. Chem. 58 (2005) 803.
[20] T.S. Lobana, Rekha, R.J. Butcher, Transition Met.Chem. 29 (2004) 291.
[21] H.G. Xeng, D.X. Zeng, X.Q. Xin, W.T. Wong, Polyhedron 16 (1997) 3499.
[22] M.B. Ferrari, G.G. Fava, M. Lanfranchi, C. Pellizzi, P. Tarasconi, Inorg. Chim. Acta 181 (1991) 253.
[23] M.B. Ferrari, A. Bonardi, G.G. Fava, C. Pellizi, P. Tarasconi, Inorg. Chim. Acta 223 (1994) 77.
[24] (a) T.S. Lobana, Rekha, R.J. Butcher, A. Castineiras, E. Bermejo, P.V. Bharatam, Inorg. Chem. 45 (2006) 1535;
(b) T.S. Lobana, Seema Paul, A. Castineiras, Polyhedron 16 (1997) 4023.
[25] S. Lhuachan, S. Siripaisarnpipat, N. Chaichat, Eur. J. Inorg. Chem. (2003) 263.
[26] G. Argay, A. Kalman, L. Parkanyl, V.M. Laovac, I.D. Braski, P.N. Radivojsa, J. Coord. Chem. 51 (2000) 9.
[27] L.A. Ashfield, A.R. Cowley, J.R. Dilworth, P.S. Donnely, Inorg. Chem. 43 (2004) 4121.
[28] Y.P. Tian, W.T. Yu, C.Y. Zhao, M.-H. Jiang, Z.G. Cai, H.K. Fun, Polyhedron 21 (2002) 1217.
[29] P. Souza, L. Sanz, V. Fernandez, A. Monge, Z. Naturoforsch B: Chem. Sci. 46 (1991) 767.
[30] C.-Y. Duan, Y.-P. Tian, C.-Y. Zhao, T.C.W. Mak, Polyhedron 16 (1997) 2857.
[31] Y.P. Tian, C.-Y. Duan, C.-Y. Zhao, X. Zhao, Inorg. Chem. 36 (1997) 1247.
[32] D.V. Garcia, A. Fernandez, J.J. Fernandez, M.L. Tornes, J.M. Origueria, J.M. Vila, H.A. Adams, J. Organomet. Chem. 595 (2000) 199.
[33] P. Dapporto, G. Demunno, A.A.G. Tomnlinsonb, J. Chem. Res. 40 (1984) 501.
[34] J.S. Casas, E.E. Castellano, J. Ellena, M.S.G. Tasende, A. Sanchez, J. Sordo, M.J. Vidarte, Inorg. Chem. 42 (2003) 2584.
[35] M. Bonamino, G. Dessy, V. Fares, L. Scaramuza, Cryst. Struct. Commun. 4 (1975) 629.
[36] R.P. John, A. Sreekanth, M.R.P. Kurup, S.M. Mobin, Polyhedron 21 (2002) 2515.
[37] D.K. Darezzeizi, N.K. Mells, D.X. West, J.V. Martinez, S. Hermande, Z. Orega, Eur. J. Inorg. Chem. (1998) 861.
[38] E. Labisbal, K.D. Haslow, K.S. Pednares, J.V. Martinez, S.H. Ortega, D.X. West, Polyhedron 22 (2003) 2831.
[39] N.T. Akinchan, R. Akinchamn, V.J. Ibok, L.P. Batlagilia, A.B. Corrada, J. Crystallogr. Spectrosc. Res. 22 (1992) 741.
[40] Y.P. Tian, W.T. Yu, M.H. Jiang, S.S.S. Raj, P. Yang, H.K. Fun, Acta Crystallogr. Sect. C: Cryst. Struct. Commun. 55 (1999) 1639.
[41] U. Abram, K. Ortner, R. Gust, K. Sommer, Dalton (2000) 735.
[42] G. Brauer, Handbook of Preparative Chemistry, 2nd ed., vol. 2, Academic Press, New York, 1965.
[43] D. Chattopadhyay, S.K. Mazumdar, T. Banerjee, S. Ghosh, T.C.W. Mak, Acta Crystallogr. C44 (1988) 1025.
[44] M.S. Garcia, J.V. Martinez, R.A. Toscano, Acta Crystallogr. C44 (1988) 1247.
[45] E. Labisbal, K.D. Haslow, A.S. Pedrares, J.V. Martinez, S.H. Ortega, D.X. West, Polyhedron 22 (2003) 2831.
[46] J.E. Huheey, E.A. Keiter, R.L. Keiter, Inorganic Chemistry: Principles of Structure and Reactivity, 4th ed., Harper Collins, New York, 1993.